Andrzej GALECKI, Arkadiusz KASZEWSKI, Lech M. Grzesiak, Bartlomiej UFNALSKI

Warsaw University of Technology, Institute of Control and Industrial Electronics

State-space current controller for the four-leg two-level grid-connected converter

Abstract. *In this paper a state-feedback current controller for four-leg grid-connected converter is presented. Two current control structures are proposed. The elementary one consists of the state regulator and a reference input matrix. The augmented one consists of the elementary structure with additional integral terms. Linear-quadratic optimization method is used to determine the controller coefficients. The developed current controller in the cascaded control structure with an outer PI DC-link voltage controller is used. Simulation results of the proposed control system are presented and discussed at the end of the paper.*

Streszczenie. *W artykule przedstawiono regulator prądu ze sprzężeniem od wektora stanu dla czterogałęziowego prostownika sieciowego. Zaproponowano dwie struktury regulacji prądu. Podstawowa zawiera regulator stanu i macierz wejścia. Rozszerzona składa się ze struktury podstawowej z dodanymi członami całkującymi. Dobór współczynników wzmocnień regulatora przeprowadzono z wykorzystaniem optymalizacji liniowo-kwadratowej. Opracowany regulator prądu współpracuje w kaskadowej strukturze regulacji z nadrzędnym regulatorem napięcia typu PI. W końcowej części artykułu przedstawiono i omówiono wyniki badań symulacyjnych.* ***(Regulator prądu ze sprzężeniem od wektora stanu dla czterogałęziowego dwupoziomowego przekształtnika sieciowego)***

Keywords: grid-connected converter, state-feedback control, linear-quadratic regulator
Słowa kluczowe: przekształtnik sieciowy, sterowanie od zmiennych stanu, regulator liniowo-kwadratowy

doi:10.12915/pe.2014.11.19

Introduction

Due primarily to an increase of non-linear devices connected to the power system, Engineers are still facing with many of the basic power quality problems such as harmonic pollution and additional power losses in the distribution system. Therefore, a three-phase active rectifier is a promising solution for power quality conditioners [1] and active filters [2]. Furthermore, due to the development of distributed generation systems including renewable energy sources there is a growing demand for voltage source converters (VSCs) connected to the four-wire grid [3].

A number of different control strategies for VSC have been proposed recently such as repetitive [4], sliding [5] predictive [6] or flatness [7] based control. Nevertheless, the voltage-oriented control (VOC) in the synchronous reference frame is still remains a well-known standard solution [8]. However, the performance of the VOC system depends of the applied current control strategy [9]. In [10], state-space current controller using pole-placement method is proposed in order to improve dynamic performance and robustness for L or LCL-filter-based system. Another approach based on Linear Quadratic Regulator (LQR) with Integral Action (LQIR) to improve dynamic performance of a three-phase three-wire shunt active power filter is presented in [11-12].

A new control structure with an outer discrete PI voltage controller and inner discrete LQ current controller for four-leg grid-connected converter (Fig. 1) is presented. The average [2], [13] model of four-leg active rectifier in dq0 reference frame is described at the beginning. In the next part current control design is extensively studied. Two current control structures in dq0 reference frame are proposed using LQ and LQI state controller, respectively. In order to track space vector grid-voltage angle φ to synchronize grid-connected converter systems with the mains, the 3-phase lock-loop based synchronous reference frame (PLL block) is used [14]. The outer PI DC-link voltage controller with an anti-windup strategy is tuned by the *systune* function (Matlab®'s tool).

System description in dq0 coordinates

The average model of a four-leg rectifier in dq0 coordinates is expressed by (1-4). This approach assumes that the v_{d}, v_{q}, v_0 is an ideal three-phase grid voltage sources and v_{dc} is ideal DC-link voltage source.

$$L\frac{\mathrm{d}i_{\mathrm{d}}}{\mathrm{d}t} = v_{\mathrm{d}} - Ri_{\mathrm{d}} + L\omega i_{\mathrm{q}} - d_d v_{\mathrm{dc}} \tag{1}$$

$$L\frac{\mathrm{d}i_{\mathrm{q}}}{\mathrm{d}t} = v_{\mathrm{q}} - Ri_{\mathrm{q}} - L\omega i_{\mathrm{d}} - d_{\mathrm{q}} v_{\mathrm{dc}} \tag{2}$$

$$(L+3L_{\mathrm{n}})\frac{\mathrm{d}i_0}{\mathrm{d}t} = v_0 - (R+3R_{\mathrm{n}})i_{\mathrm{o}} - d_0 v_{\mathrm{dc}} \tag{3}$$

$$C_{\mathrm{dc}}\frac{\mathrm{d}v_{\mathrm{dc}}}{\mathrm{d}t} = \frac{3}{2}(d_{\mathrm{d}}i_{\mathrm{d}} + d_{\mathrm{q}}i_{\mathrm{q}}) + 3d_0 i_0 - i_{\mathrm{load}} \tag{4}$$

The R, R_{n}, L, L_{n}, C_{dc} are respectively resistances and inductances of phase and neutral filter legs and DC-link capacitance. The load R_{load} current connected to the DC-link is named as i_{load}. The model given by (1-4) is nonlinear because of the product of the duty cycles d_{d}, d_{q}, d_0 and the grid currents $\mathrm{i_d}$, $\mathrm{i_q}$, $\mathrm{i_0}$ or $\mathrm{v_{dc}}$ respectively. The average circuit model is presented in Fig. 2. In order to obtain the state-space model with all listed state variables the linearization process is needed [13].

State-space model for current control design

For the state-space current controller design the selected equations (1-3) are used. This way the linearization problem can be reduced to $v_{\mathrm{dc}} = \mathrm{const.}$ The state-space model is obtained taking into account that $v_{\mathrm{dc}} = V_{\mathrm{dc}}$. Measurement gain of the grid current k_{i} are incorporated into the state-space model given in (5).

$$\frac{\mathrm{d}\mathbf{x}}{\mathrm{d}t} = \mathbf{A}\mathbf{x} + \mathbf{B}\mathbf{u} + \mathbf{E}\mathbf{v} \tag{5}$$

where

$$\mathbf{A} = \begin{bmatrix} -\frac{R}{L} & \omega & 0 \\ -\omega & -\frac{R}{L} & 0 \\ 0 & 0 & -\frac{R+3R_{\mathrm{n}}}{L+3L_{\mathrm{n}}} \end{bmatrix}, \quad \mathbf{x} = \begin{bmatrix} i_{\mathrm{d}}^{\mathrm{m}} \\ i_{\mathrm{q}}^{\mathrm{m}} \\ i_0^{\mathrm{m}} \end{bmatrix} \tag{6}$$

(7) $$\mathbf{B}=\begin{bmatrix} -\frac{V_{dc}}{L}k_i & 0 & 0 \\ 0 & -\frac{V_{dc}}{L}k_i & 0 \\ 0 & 0 & -\frac{V_{dc}}{L+3L_n}k_i \end{bmatrix},\ \mathbf{u}=\begin{bmatrix} d_d \\ d_q \\ d_0 \end{bmatrix}$$

(8) $$\mathbf{E}=\begin{bmatrix} \frac{1}{L}k_i & 0 & 0 \\ 0 & \frac{1}{L}k_i & 0 \\ 0 & 0 & \frac{1}{L+3L_n}k_i \end{bmatrix},\ \mathbf{v}=\begin{bmatrix} v_d \\ v_q \\ v_0 \end{bmatrix}$$

There are three measurement grid currents i_d^m, i_q^m, i_0^m as state variables , three duty cycle d_d, d_q and d_0 as inputs and three grid voltages v_d, v_q, v_0 as disturbances collected sequentially in the **x, u** and **v** vectors and three matrices: **A** – the state matrix, **B** – the control matrix and **E** – the disturbance matrix. The coupling terms ω have been taken into account in the state current controller design, in contrast to structure with PI controller, where to the output of the controller a simple forward decoupling voltage is usually added. The output equation is defined as: $\mathbf{y}=\mathbf{Cx}$, where $\mathbf{C}$ is the identity matrix.

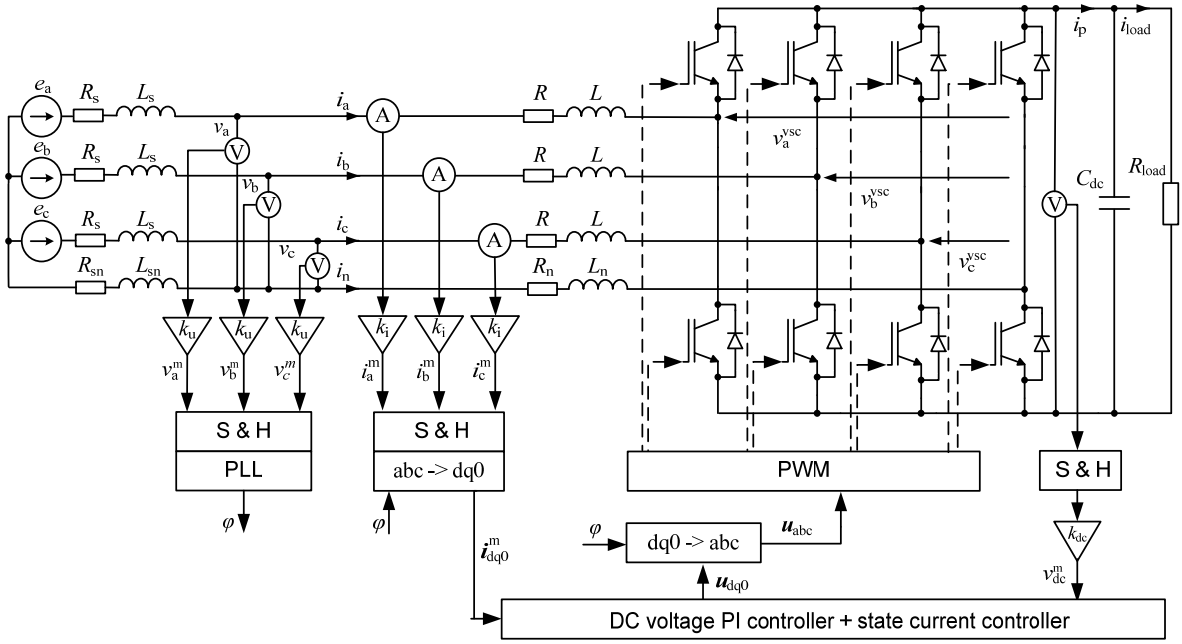

Fig. 1. Schematic diagram of a four-leg PWM converter connected to the grid

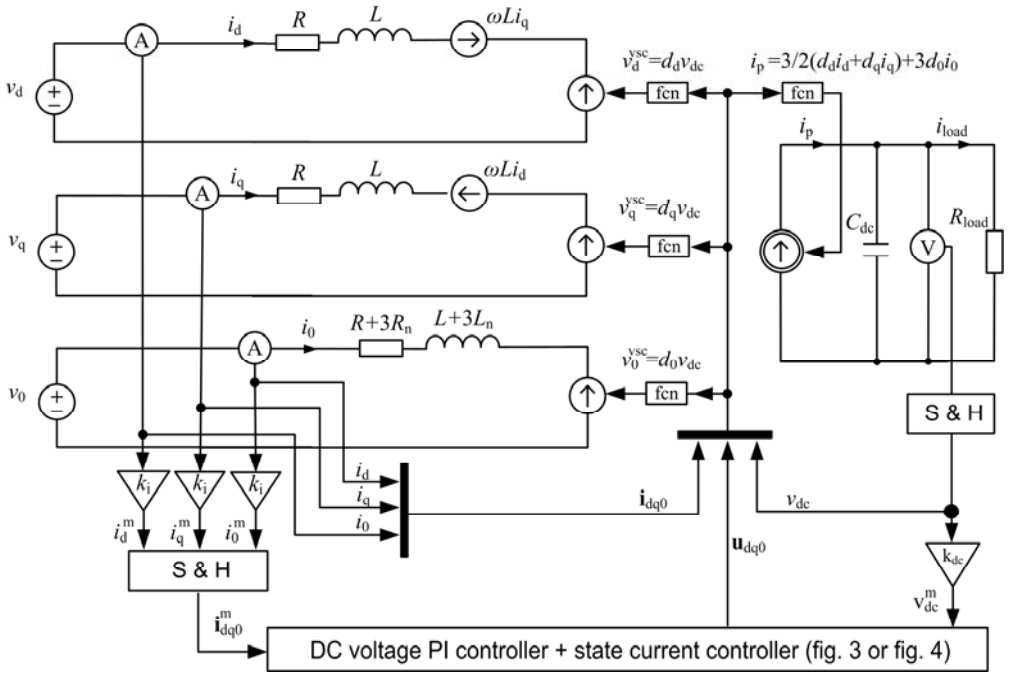

Fig. 2. Average model of a four-leg PWM converter in dq0 coordinates

The new differential equations (9) have been added in order to eliminate a constant type of errors in steady-state:

$$(9)\qquad \frac{\mathrm{d}p_{\mathrm{d}}}{\mathrm{d}t}=i_{\mathrm{d}}^{\mathrm{m}}-i_{\mathrm{d}}^{\mathrm{ref}},\ \frac{\mathrm{d}p_{\mathrm{q}}}{\mathrm{d}t}=i_{\mathrm{q}}^{\mathrm{m}}-i_{\mathrm{q}}^{\mathrm{ref}},\ \frac{\mathrm{d}p_{0}}{\mathrm{d}t}=i_{0}^{\mathrm{m}}-i_{0}^{\mathrm{ref}}$$

The state-space augmented model is given bellow

$$10)\qquad \frac{\mathrm{d}\mathbf{x}_{\mathrm{I}}}{\mathrm{d}t}=\mathbf{A}_{\mathrm{I}}\mathbf{x}_{\mathrm{I}}+\mathbf{B}_{\mathrm{I}}\mathbf{u}_{\mathrm{I}}+\mathbf{E}_{\mathrm{I}}\mathbf{v}$$

$$(11)\qquad \mathbf{A}_{\mathrm{I}}=\begin{bmatrix}\mathbf{A} & 0\\ \mathbf{A_p} & 0\end{bmatrix},\ \mathbf{x}_{\mathrm{I}}=\begin{bmatrix}\mathbf{x} & \mathbf{p}\end{bmatrix}^{T}$$

$$(12)\qquad \mathbf{B}_{\mathrm{I}}=\begin{bmatrix}\mathbf{A}\\ \mathbf{0}\end{bmatrix},\ \mathbf{u}_{\mathrm{I}}=\begin{bmatrix}d_{\mathrm{d}} & d_{\mathrm{q}} & d_{0}\end{bmatrix}^{T}$$

$$(13)\qquad \mathbf{E}_{\mathrm{I}}=\begin{bmatrix}\mathbf{E}\\ \mathbf{0}\end{bmatrix},\ \mathbf{v}=\begin{bmatrix}v_{\mathrm{d}} & v_{\mathrm{q}} & v_{0}\end{bmatrix}^{T}$$

where:

$$(14)\qquad \mathbf{A}_{\mathbf{p}}=\begin{bmatrix}1 & 0 & 0\\ 0 & 1 & 0\\ 0 & 0 & 1\end{bmatrix}\ \text{and}\ \mathbf{p}=[p_{\mathrm{d}}\quad p_{\mathrm{q}}\quad p_{0}]^{T}$$

There are new augmented matrices: $\mathbf{A}_{\mathrm{I}}$ – the augmented state matrix, $\mathbf{B}_{\mathrm{I}}$ – the augmented control matrix, $\mathbf{E}_{\mathrm{I}}$ – the augmented disturbance matrix and new augmented state vector $\mathbf{x}_{\mathrm{I}}$ consist of $\mathbf{x}$ and $\mathbf{p}$.

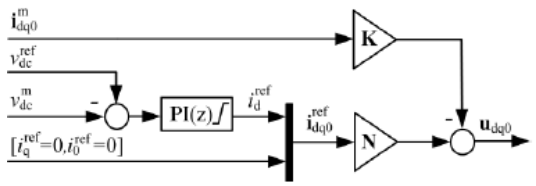

Fig. 3. Converter control structure based on LQ current controller and PI DC-link voltage controller

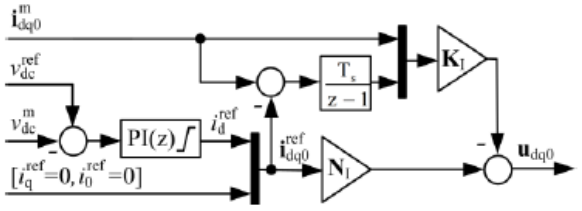

Fig. 4. Converter control structure based on LQI current controller and PI DC-link voltage controller

Full-state-feedback current controller design

The state-feedback current controller in the dq0 rotating frame has been designed using the elementary (5) and next the augmented model (10). For this purpose, the LQR method in the discrete model is applied using *lqrd* Matlab®'s function. Firstly the continuous-time model is discretized. For the LQ current controller the state-feedback matrix $\mathbf{K}$ is calculated such that the discrete state-feedback low $\mathbf{u}(k)=-\mathbf{K}\mathbf{x}(k)$ minimizes a discrete cost function:

$$(15)\qquad J=\sum_{k=0}^{\infty}(\mathbf{x}^{T}(k)\mathbf{Q}_{0}\mathbf{x}(k)+\mathbf{u}^{T}(k)\mathbf{R}\mathbf{u}(k))$$

For the LQI current controller the state-feedback augmented matrix $\mathbf{K}_{\mathrm{I}}$ is calculated such that the discrete state-feedback low $\mathbf{u}_{\mathrm{I}}(k)=-[\mathbf{K}_{0}\quad \mathbf{K}_{\mathbf{p}}]\mathbf{x}_{\mathrm{I}}(k)=-\mathbf{K}_{\mathrm{I}}\mathbf{x}_{\mathrm{I}}(k)$ minimizes a discrete cost function:

$$(16)\qquad J_{I}=\sum_{k=0}^{\infty}(\mathbf{x}_{\mathrm{I}}^{T}(k)\begin{bmatrix}\mathbf{Q}_{0} & \mathbf{0}\\ \mathbf{0} & \mathbf{Q}_{\mathbf{p}}\end{bmatrix}\mathbf{x}_{\mathrm{I}}(k)+\mathbf{u}_{\mathrm{I}}^{T}(k)\ \mathbf{R}\mathbf{u}_{\mathrm{I}}(k))$$

The $\mathbf{Q}_{0}$, $\mathbf{Q}_{\mathbf{p}}$ and $\mathbf{R}$ matrices are chosen by check and guess method and assuming the diagonal structure. The control structure is scaled to unity so the Bryson's [14] rule is taken into account automatically.

Reference input matrix

The reference input $\mathbf{N}$ matrix is calculated for converter control structure based on LQ current controller (Fig. 3) as $\mathbf{N}=\mathbf{N_u}+\mathbf{K}\mathbf{N_x}$, in order to ensure unity closed-loop steady state gain, assuming that disturbances are equated to zero.

$$(17)\qquad \begin{bmatrix}\mathbf{N_x}\\ \mathbf{N_u}\end{bmatrix}=\begin{bmatrix}\mathbf{A}_{\mathrm{d}}-\mathbf{I} & \mathbf{B}_{\mathrm{d}}\\ \mathbf{C}_{\mathrm{d}} & \mathbf{0}\end{bmatrix}^{-1}\begin{bmatrix}\mathbf{0}\\ \mathbf{I}\end{bmatrix}$$

The $\mathbf{A}_{\mathrm{d}}$, $\mathbf{B}_{\mathrm{d}}$ and $\mathbf{C}_{\mathrm{d}}$ are the discrete equivalent of matrices $\mathbf{A}$, $\mathbf{B}$ and $\mathbf{C}$. The $\mathbf{N_x}$ is the identity matrix. For augmented current control structure the $\mathbf{N_u}$ matrix is replaced by integral terms [14]. Therefore, for converter control structure based on LQI current controller (Fig. 4), the reference input matrix $\mathbf{N}_{\mathrm{I}}=\mathbf{K}_{0}\mathbf{N_x}$.

DC voltage controller design

For DC voltage regulation, an outer feedback control loop with PI regulator is used. In order to calculate controller gain, symmetrical optimum can be used [15]. In this paper, the regulator is tuned by the *systune* Matlab®'s function [16] using average model (Fig. 2). For specifying the desired behavior of the tuned control system a control design requirements must be specified. The TuningGoal.Rejection class [17] is used to specify the minimum attenuation profile expected at a $i_{\mathrm{d}}^{\mathrm{ref}}$ point. The controller output value is kept within a maximum limits. Therefore, the reference current $i_{\mathrm{d}}^{\mathrm{ref}}$ is limited.

Simulation result

Performance of the system under step of load from 0 to 100% and back to 0 is presented in Fig. 5 and 6 for LQ and LQI current controller, respectively. In both cases, the grid voltage, grid current and DC-link voltage waveforms are presented in dq0 reference frame.

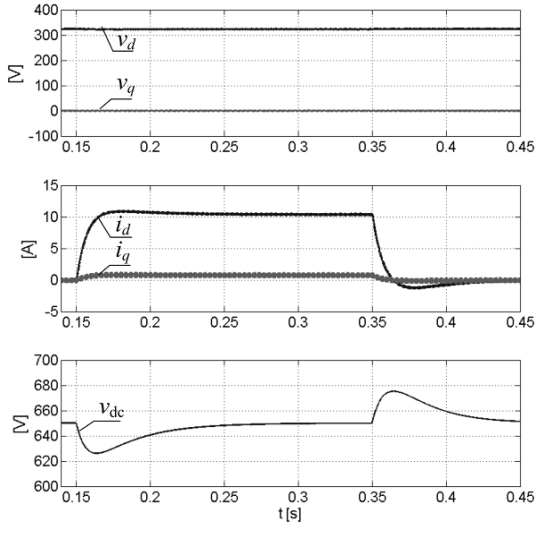

Fig. 5. Performance of the system with LQ current controller under 5 kW step of load from 0 to 100% and back to 0

From time point 0.15 s to 0.3 s the 5 kW load R_{load} is connected. The i_{d} current with 0.5 A overshot after R_{load} is connected and 1 A overshot after R_{load} is disconnected.

Tuned DC-link voltage controller provides 1.5% overshoot and the settling time about 0.1 s on the v_{dc}.

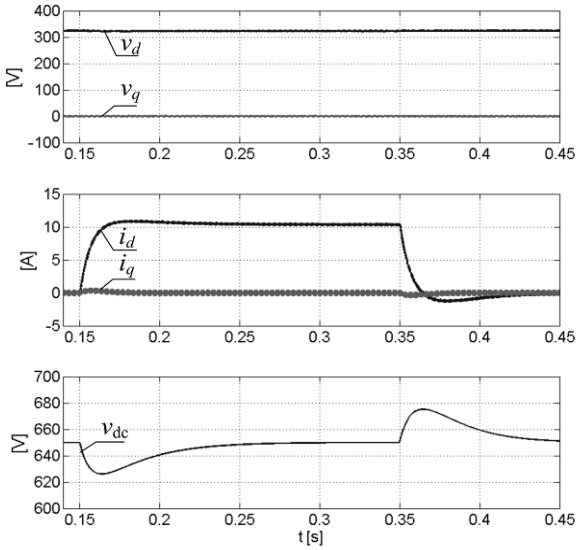

Fig. 6. Performance of the system with LQI current controller under 5 kW step of load from 0 to 100% and back to 0

Comparison of the system performance with LQ and LQI current controller in steady-state is presented in Figure 7. In the case when integral term is not included phase shift between grid voltage and current is 9.17°, so cos(Φ)=0.987.

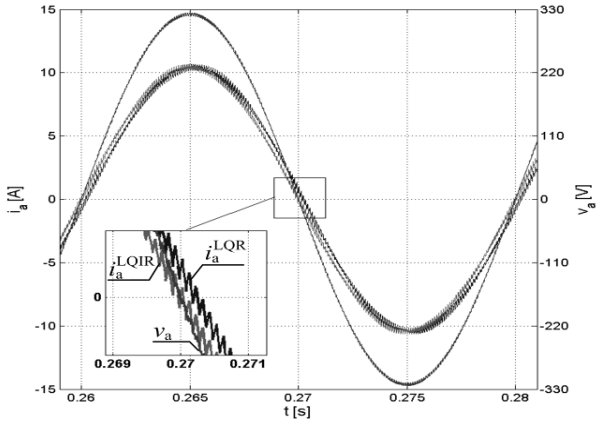

Fig. 7. Performance of the system with LQ and LQI current controller in steady-state

Conclusion

State-space current controller for four-leg grid-connected converter based on linear-quadratic optimization method has been presented. To obtain a unity power factor the augmented structure with additional integral terms has been proposed. Performance of the control system with the inner state current controller and the outer PI DC-link voltage controller have been verified in simulation studies. Hence, in order to achieve high control performance the straightforward controller tuning for a particular system setting has been presented.

Appendix

Simulation parameters:

Nominal phase-neutral grid voltage	V=325 V
Nominal DC-link voltage	V_{dc}=650 V
Nominal pulsation of the grid voltage	ω=100pi s^{-1}
Switching/sampling time	T_s =0.0001 s
Inductance of the input filter	L=4 mH
Resistance of the DC-link capacitor	R=0.5 Ω
Capacitance of the DC-link capacitor	C_{dc}=1.5 mF
DC load parameter	R_{load} =84 Ω
Inductance of the grid	L_s=L_{sn}=100 μH
Resistance of the grid	R_s=R_{sn}=0.1 Ω
Measurement gain of the grid voltage	k_u=1/325 V^{-1}
Measurement gain of the grid current	k_i=1/25 A^{-1}
Measurement gain of the DC-link voltage	k_{dc}=1/650 V^{-1}

The weighting matrices in (15) and (16) for current controller design: $\mathbf{Q}_0$ = diag([10^{-5}, 10^{-5}, 10^{-5}]), $\mathbf{Q}_p$ = diag ([10^5, 10^5, 10^5]), $\mathbf{R} = \mathbf{I}_{3x3}$

This study was financed from funds for statutory activity of Electrical Drive Division, Institute of Control and Industrial Electronics, Faculty of Electrical Engineering Warsaw University of Technology.

REFERENCES

[1] Silva S.A.O., Modesto R.A., Goedtel A., Nascimento C.F., Compensation Algorithms Applied to Power Quality Conditioners in Three-Phase Four-Wire Systems, in proc. of *IEEE International Symposium on Industrial Electronics*, 2010, pp. 730-735

[2] Rodriguez P., Luna A., Teodorescu R., Blaabjerg F., Liserre M., Control of a Three-phase Four-wire Shunt-Active Power Filter Based on DC-link Energy Regulation, in proc. of *IEEE Intern. Conf. Optimal. of Electrical and Electronic Equip.* 2008, pp 227-234

[3] Sedlak M., Stynski S., Kazmierkowski M.P., Malinowski M., Three-level four-leg flying capacitor converter for renewable energy sources, *Przeglad Elektrotechniczny*, 2012, vol. 12a

[4] Escobar G., Martinez P.R., Leyva-Ramos J. and Mattavelli P., Power factor correction with an active filter using a repetitive controller, in proc. of *IEEE International Symposium on Industrial Electronics*, 2006, Vol.2, pp. 1394-1399

[5] Mendalek N., Al-Haddad, K., Kanaan H.Y., Hassoun G., Sliding mode control of three-phase four-leg shunt active power filter, in proc. of *IEEE Power Electr. Spec. Conf.* 2008, pp. 4362 – 4367.

[6] Antoniewicz P., Kazmierkowski M.P., Predictive direct power control of three-phase boost rectifier, *Bulletin of Polish Academy of Science, Technical Sciences*, 2006, Vol. 54, No. 3

[7] Dannehl J. and Fuchs F., Flatness-based voltage-oriented control of three phase PWM rectifiers, in proc. 13th Int. *Power Electron. Motion Control Conf.,* 2008, pp. 444–450.

[8] Kazmierkowski M.P., Cichowlas M., Comparison of current control techniques for PWM rectifiers, in proc. of *IEEE International Symposium on Industrial Electronics*, 2002, Vol. 4, pp 1259-1263.

[9] Bobrowska M., Rafal K., Milikua H., Kazmierkowski M.P., Improved Voltage Oriented Control of AC-DC converter under balanced and unbalanced grid voltage dips, in proc. of *IEEE International Conf. EUROCON*, 2009, pp. 772-776

[10] Dannehl J., Fuchs F., and Thgersen P., PI state space current control of grid-connected PWM converters with LCL filters, *IEEE Trans. Power Electron*., 2010, vol. 25, no. 9, pp. 2320–2330

[11] Kedjar B. and Al-Haddad K., LQ control of a three-phase four-wire shunt active power filter based on three-level NPC inverter, in proc. of *Canadian Conference on Electrical and Computer Engineering CCECE*, 2008, pp. 001279-001302

[12] Kedjar B., Kanaan H.Y., Al-Haddad K., Vienna Rectifier With Power Quality Added Function, *IEEE Transactions on Industrial Electronics*, 2014, vol. 61, pp. 3847-3856.

[13] Kanaan H.Y., Hayek A. and Al-Haddad K., Small-signal average modeling, simulation and carrier-based linear control of a three-phase four-leg shunt active power filter, in proc. of *IEEE Intern. Electric Machines and Drives Conf*., 2007, pp. 601-60

[14] Franklin G.F. and Powell J.D., Digital Control of Dynamic Systems, *Addison-Wesley*, London,1980

[15] Kazmierkowski M.P., Krishnan R., Blaabjerg F., Control in Power Electronics, *Academic Press*, Oxford, UK, 2002

[16] http://www.mathworks.com/help/robust/gs/tuning-control-systems-with-systune.html (28.04.2014)

[17] http://www.mathworks.com/help/robust/gs/pid-tuning-for-setpoint-tracking-vs-disturbance-rejection.html (28.04.2014)

***Autorzy**: mgr inż. Andrzej Gałecki, dr inż. Arkadiusz Kaszewski, prof. dr hab. inż. Lech M. Grzesiak, dr inż. Bartłomiej Ufnalski, Politechnika Warszawska, Instytut Sterowania i Elektroniki Przemysłowej, ul. Koszykowa 75, 00-662 Warszawa, E-mail: andrzej.galecki@ee.pw.edu.pl*